Olander, D. R., "Simultaneous Mass Transfer and Equilibrium Chemical Reaction," *AIChE J.*, **6**, 2, 233 (1960).
Peaceman, D. W., "Liquid-Side Resistance in Gas Absorption with and without Chemical Reaction," Sc. D. Thesis, Mass. Inst. Tech., Cambridge, MA (1951).
Rabe, A. E., and J. F. Harris, "Vapor Liquid Equilibrium Data for the Binary System, Sulfur Dioxide and Water," *J. Chem. Engr. Data*, **8**, 333 (1963).
Rochelle, G. T., and C. J. King, "The Effects of Additives on Mass Transfer in $CaCO_3$ or CaO Slurry Scrubbing of SO_2 from Waste Gases", *Ind. Eng. Chem. Fund.*, **16**, 67 (1977).
Rochelle, G. T., and C. J. King, "Alternatives for Stack Gas Desulfurization by Throwaway Scrubbing," *Chem. Eng. Prog.*, p. 65 (February, 1978).
Tartar, H. V., and H. H. Garretson, "The Thermodynamic Ionization Constants of Sulfurous Acid at 25°C," *JACS*, **63**, 808 (1941).
Wasag, T., J. Galka, and M. Fraczak, "Effects or Organic Acids on the Kinetics of SO_2 Absorption," *Air Conservation*, **9**, 16 (1975).

Manuscript received November 26, 1979; revision received March 19, and accepted May 15, 1981

Analysis of Annular Bed Reactor for Methanation of Carbon Monoxide

M. E. DAVIS
and
JOHN YAMANIS

Department of Chemical Engineering
University of Kentucky
Lexington, KY 40506

A new reactor configuration, the annular bed reactor, is mathematically modeled to assess its capabilities as a CO methanation reactor. The results show that the reactor offers excellent temperature control characteristics and negligible pressure drop, and that it is a promising configuration for this as well as other reaction systems.

SCOPE

It was the purpose of the present work to introduce a new reactor configuration, the annular bed reactor (ABR), and to assess its capabilities for use as a methanation reactor. This reactor is made up of an annular catalyst bed of very small particles next to the heat transfer surface with the inner core of the annulus packed with large, inert spheres. The main fluid flow is in the axial direction through the core where the inert packing promotes radial transport to the catalyst bed. The annular bed reactor is susceptible to deactivation as the tube wall reactor. However, the effect of deactivation on the overall reactor performance is less pronounced (in the same time span) in the ABR due to the large amount of catalyst.

CONCLUSIONS AND SIGNIFICANCE

Using a feed mixture of 25% carbon monoxide in hydrogen at 290–310°C and 2.17 MPa, the reactor model predicted near-isothermal, near-isobaric behavior in that maximal axial and radial temperature gradients were 10 and 4°C, respectively, while the pressure gradients never exceeded 1% of the inlet pressure. Large inert particles in the core increased exit conversion due to enhancement of radial transport processes. The reactor behavior was sensitive to the catalytic bed thickness. For a given reactor length, the exit conversion increased with increased bed thickness, but for a given mass of catalyst it was found that a longer thin bed outperformed a shorter thick bed due to the increased residence time. Increasing residence times, i.e., decreasing Reynolds numbers, were found to increase exit conversions and axial temperature gradients.

From the simulations presented in this work it can be seen that the annular bed reactor is a very promising configuration for the carbon monoxide methanation reaction.

INTRODUCTION

Due to the escalating demand for natural gas and the growing shortage of supply, there is considerable interest in the production of substitute natural gas (SNG) from coal. None of the state-of-the-art coal gasification processes can produce pipeline quality gas unless the gasifier effluent is subjected to methanation. The overall reactions of the methanation step are:

$$CO + 3H_2 = CH_4 + H_2O,\ \Delta H_r = -49.3\ \text{kcal/mol}, \quad (1)$$

$$CO_2 + 4H_2 = CH_4 + 2H_2O,\ \Delta H_r = -39.5\ \text{kcal/mol}. \quad (2)$$

Owing to the highly exothermic nature of the reactions, temperature control of methanation reactors becomes difficult. Various reactor configurations such as the parallel plate and the coated tube wall (Haynes et al., 1977; Penline et al., 1979) have been proposed as methanation reactors because of their novel methods of heat removal. Penline et al. (1979) were able to successfully methanate high concentrations of CO (25% or less) in a coated tube wall reactor (TWR) but observed severe deactivation with feed sulfur concentrations around 66 ppb.

Another reactor system, the parallel passage reactor (DeBruijn et al., 1978), appears to be a likely candidate for accomplishing

Correspondence concerning this paper should be addressed to J. Yamanis.
M.E. Davis is presently at the Virginia Polytechnic Institute, Blacksburg, VA 24061.
0001-1541-82-4996-0266-$2.00

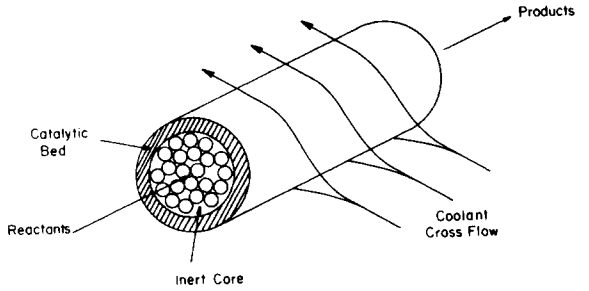

Figure 1. Schematic of annular bed reactor tube.

methanation reactions. The parallel passage reactor (PPR) contains shallow beds of catalyst separated from narrow channels by wire screens. Compared to the TWR the PPR possesses a relatively thick layer of catalyst and so poisoning would probably have less effect, although heat removal would be expected to be less efficient than in the TWR. DeBruijn et al. (1978) successfully methanated low concentrations of CO_2 (3% or less) in a rectangular shaped laboratory scale PPR. Their reactor remained isothermal and their reactor model agreed well with most but not all of their experimental data. Davis et al. (1981) showed that this incomplete agreement was due to a redundant assumption in the reactor model, and that complete agreement with the data was possible by the removal of that assumption.

In a PPR transport of reactants to the catalyst bed is governed by molecular diffusional processes at right angles to the main flow. In order to improve the transport characteristics of such a reactor, the void space could be packed with large inert packing that improves transport to the catalyst bed while offering little resistance to flow. To this end, it was proposed by Davis et al. (1981) to construct a reactor in the form of a bundle heat exchanger, the tubes of which were to be packed with small size catalyst particles in the annular space between the wall and the central core, the latter being packed with large inert spheres, a single tube schematic of which is shown in Figure 1. The two particle beds are separated by an inert screen, and the main flow is in the axial direction through the core while reactants are transported to the catalyst bed by radial dispersion processes. This reactor configuration was termed an annular bed reactor (ABR), and by using the experimental conditions of DeBruijn et al. (1978), Davis et al. (1981) were able to show improvements in conversion brought about by packing the inner core.

It was the purpose of the present work to examine the nonisothermal behavior of the ABR for the faster and more pertinent reaction of the methanation of carbon monoxide.

REACTOR MODEL

Assuming the effects of temperature, pressure, and volume change due to reaction on the concentration and the average axial velocity to be negligible and using mean physical properties, the ABR is described by Eqs. 3 and 4 which are in dimensionless form:

$$\delta_1 S_r \frac{\partial f}{\partial z} = \left[\frac{A_m A_n}{\mathrm{ReSc}}\right] \frac{1}{r} \frac{\partial}{\partial r}\left(r D_r \frac{\partial f}{\partial r}\right) + \delta_2 \left[\frac{A_n/A_m}{\mathrm{ReSc}}\right] \frac{\partial}{\partial z}\left(D_a \frac{\partial f}{\partial z}\right) + \delta_3 \left[\frac{A_m A_n}{\mathrm{ReSc}}\right] \phi^2 R, \quad (3)$$

$$\delta_1 S_r \frac{\partial t}{\partial z} = \left[\frac{A_m A_n}{\mathrm{RePr}}\right] \frac{1}{r} \frac{\partial}{\partial r}\left(r K_r \frac{\partial t}{\partial r}\right) + \delta_2 \left[\frac{A_n/A_m}{\mathrm{RePr}}\right] \frac{\partial}{\partial z}\left(K_a \frac{\partial t}{\partial z}\right) + \delta_3 \left[\frac{A_m A_n}{\mathrm{RePr}}\right] \beta \phi^2 R, \quad (4)$$

where δ_1, δ_2, and δ_3 signify the presence or absence of a term in the above equations for a given region as shown in Table 1. For solution, Eqs. 3 and 4 must be complimented by the appropriate boundary conditions which are given by:

TABLE 1. DELTA VALUES FOR THREE REACTOR REGIONS

		Core	Screen	Bed
δ_1		1	0	0
δ_2	Parabolic	0	0	0
	Elliptic	1	1	1
δ_3		0	0	−1

$$\frac{\partial f}{\partial r} = 0 \frac{\partial t}{\partial r} = 0 \qquad \text{at } r = 0, \quad (5)$$

$$D_r^T \frac{\partial f}{\partial r}\bigg|_{r_T} = D_r^{sc} \frac{\partial f}{\partial r}\bigg|_{r_T} K_r^T \frac{\partial t}{\partial r}\bigg|_{r_T} = K_r^{sc} \frac{\partial t}{\partial r}\bigg|_{r_T} \qquad \text{at } r = r_T, \quad (6)$$

$$D_r^{sc} \frac{\partial f}{\partial r}\bigg|_{r_B} = D_r^B \frac{\partial f}{\partial r}\bigg|_{r_B} K_r^{sc} \frac{\partial t}{\partial r}\bigg|_{r_B} = K_r^B \frac{\partial t}{\partial r}\bigg|_{r_B} \qquad \text{at } r = r_B, \quad (7)$$

$$\frac{\partial f}{\partial r} = 0 K_r \frac{\partial t}{\partial r} = U_c(t_c - t) \qquad \text{at } r = 1, \quad (8)$$

$$\frac{\partial t}{\partial z} = 0 \frac{\partial t}{\partial z} = 0 \qquad \text{at } z = 1, \quad (9)$$

$$\text{initial conditions for } f \text{ and } t \qquad \text{at } z = 0, \quad (10)$$

where the transport coefficients in Eqs. 6–9 and the initial conditions are discussed later.

The two sets of values for δ_2 listed in Table 1 arise from inclusion or not of axial diffusion or dispersion processes. When these processes are not included the reactor is described by a set of mixed-type, partial differential equations (one of which is parabolic and thus the reactor problem will be referred to as parabolic) while when the dispersion processes are included the set of equations are elliptic. The present discussion is restricted to the parabolic problem for which conditions 9 are not needed. Results and discussion pertaining to the elliptic problem will appear in another publication.

From the conditions listed for δ_1 and δ_2 it can be seen that axial flow is assumed to occur only in the central core, and that the reaction occurs only in the catalytic bed. Note that the Reynolds number is based on the inert particle diameter, the Thiele modulus, ϕ, is based on the reaction rate at inlet conditions and inlet concentration, and the Prater number, β, is based on inlet concentration and temperature.

Since the axial velocity is assumed to go to zero at r_T (core-screen interface), heat and mass transport from the core to the bed is molecular as indicated by Eqs. 6–7. At the inside surface of the reactor wall ($r = 1$) heat is conducted through the wall and convectively carried away at the outer surface by the coolant. The overall heat transfer coefficient includes the combined resistances of the wall and the convective film coefficient. The bulk coolant temperature is held constant throughout the length of the reactor and is set equal to the inlet reactant gas temperature, T_o.

TRANSPORT COEFFICIENTS

Inner Core

When a number of particles are randomly placed in a container the result is a inhomogeneous medium characterized by void spaces. The distribution of void space is dependent upon d_T/d_P and independent of axial dimensions. Schwartz and Smith (1953) found that the velocity across the diameter of a packed bed is not uniform, unless $d_T/d_P > 30$, due to the significant effect of the increased void space near the wall where the particles are locally ordered. Fahien and Stankovic (1979) have correlated experimental data on point velocities and established an equation (Eq. A.1 given in the Appendix for completeness) for predicting local axial velocities in packed beds.

There are considerable data on average radial Peclet numbers in the literature but data on local Peclet numbers are rather limited (Schertz and Bischoff, 1967; Fahien and Smith, 1955). However,

equations for predicting the local radial dispersion coefficient for mass, E, (Eq. A.8) and for heat, k, (Eq. A.12) were recently proposed by Ahmed and Fahien (1980) who successfully modeled the epxerimental SO_2-oxidation reactor of Schuler et al. (1952) by using these equations. More recently, Davis (1981) showed that the pure heat transfer data of DeWasch and Froment (1971) could be adequately described by a packed reactor model involving transport coefficients given by the aforementioned equations. Based on the success of these applications, the above predictive equations for the transport coefficients were used to evaluate the behavior of the annular bed reactor for which:

$$D_r = \frac{\text{ReSc}}{\langle \text{Pe} \rangle} E, \qquad 0 \le r \le r_T, \tag{11}$$

$$K_r = \langle k \rangle \, k/k_{\text{mix}}, \qquad 0 \le r \le r_T, \tag{12}$$

where

$$\langle \text{Pe} \rangle = 9[1 + 4.85\alpha^{-2}], \tag{13}$$

and was obtained from Fahien and Smith (1955).

Screen and Bed

Since no axial flow is accounted for in the screen and bed, transport in these regions is purely molecular, i.e., molecular mass diffusion and heat conduction, so that $D_r = D_a$ and $K_r = K_a$, where:

$$D_r^i = \tau_i, \qquad i = \text{screen or bed}, \tag{14}$$

$$K_r = \text{voidage weighted thermal conductivity}/k_{\text{mix}}. \tag{15}$$

INITIAL CONDITIONS

The boundary conditions at the reactor inlet ($z = 0$) have not been specified in Eq. (10) because different conditions may be specified there depending on the type of P.D.E. used and the condition that may be specified at the boundary of the catalytic bed.

As mentioned earlier, when axial dispersion processes are neglected, Eqs. 3 and 4 become a set of mixed-type, coupled, nonlinear partial differential equations, the core equation being of the parabolic type. The most appropriate initial condition for the inner core is

$$f = 1 \qquad t = 1 \qquad \text{at } z = 0, \qquad \text{for } 0 \le r \le r_T. \tag{16}$$

The initial condition at the catalytic bed boundary depends on whether reaction is considered to occur at this plane. If no reaction occurs, the concentration and temperature profiles are flat given by:

$$f = 1 \qquad t = 1 \qquad \text{at } z = 0, \qquad \text{for } r_T \le r \le 1. \tag{17}$$

If reaction is considered to occur, the initial condition for this boundary is given by

$$f = f(r) \qquad \text{at } z = 0, \qquad \text{for } r_B \le r \le 1, \tag{18}$$

where $f(r)$ is a radial function obtained by solving the problem

$$\frac{\partial^2 f}{\partial r^2} + \frac{1}{r}\frac{\partial f}{\partial r} = \frac{\phi^2}{D_r} R, \tag{19}$$

$$f = 1 \qquad \text{at } r = r_B, \tag{20}$$

$$\frac{\partial f}{\partial r} = 0 \qquad \text{at } r = 1, \tag{21}$$

assuming the temperature profile is flat at that boundary.

The effects of the above two sets of boundary conditions for f and t at $z = 0$ on reactor performance have been assessed and are discussed later.

TABLE 2. CATALYST STRUCTURE PARAMETERS

θ_{cat}	0.4
τ_{cat}	2.0
a_m	3.5 nm

REACTION KINETICS

There has been much discussion over the reaction rate functions reported for the CO methanation. Vannice (1976) has reported turnover numbers for various commercial and doped nickel catalysts. His results compare favorably with those of Dalla Betta et al. (1974). Recently Goodman et al. (1980) reported turnover numbers and activation energies for pure nickel crystals, and their results compare reasonably well with the data of Vannice. It is therefore felt that the expressions for the reaction rate reported by Vannice are representative of intrinsic kinetics. For a 5% Ni/η-Al_2O_3 catalyst, Vannice described the reaction rate by:

$$\mathcal{R}_{\text{CO}} = \rho_B K_o C_{\text{H}_2}^{0.8} C_{\text{CO}}^{-0.3}, \tag{22}$$

$$473 \le T \le 573,$$

$$\text{H}_2/\text{CO} = 3,$$

$$\%\ \text{CO} = 25,$$

$$P = 101\ \text{kPa},$$

where

$$K_o = 7.06 \times 10^3 \exp(-23{,}400/R_g T)(R_g T)^{0.5}. \tag{23}$$

In modeling the CO methanation, Eq. 22 has been extrapolated to higher pressures. Jarvi et al. (1980) showed that the total pressure dependence of the CO methanation reaction on Ni/Al_2O_3 catalysts has an order of 0.4–0.6 for pressures in the range of 140 to 2,500 kPa, which is in good agreement with the 0.5 order of Eq. 22.

Since no catalyst structure parameters were presented by Vannice, the data listed in Table 2, which are average values for nickel based catalysts (Satterfield, 1970), were used. Single catalyst pellet behavior was modeled using a dusty-gas flux model. In order to eliminate intraparticle diffusion limitations for 25–75% conversion of 25% CO in H_2 mixture at $T = 573$ K, $P = 2.17$ MPa, the particle diameter, d_P^{cat}, must be smaller than 1.0 mm (Davis, 1981).

The ABR by its design allows the catalytic bed to be made up of very small particles without undue pressure drop. A catalytic pellet diameter of 1.0 is therefore not unreasonable and was used in the subsequent analysis of the annular bed reactor.

NUMERICAL TECHNIQUES

The parabolic set of differential equations was solved by two methods, namely, an extrapolated Crank-Nicolson (smoothed; Lindberg, 1971; Lawson and Morris, 1978), and a backward finite difference technique, both achieving the same solution. These numerical methods were successfully used to predict the experimentally determined behavior of the parallel passage reactor (DeBruijn et al., 1978) and the isothermal annular bed reactor for methanation of carbon dioxide (Davis et al., 1981). The parameter space which could be studied using the parabolic system of equations was confined to the subspace which produced positive finite concentrations at the wall.

RESULTS

In all the data presented below, radial thermal gradients were practically non-existent with maximum values of 4 K, while axial

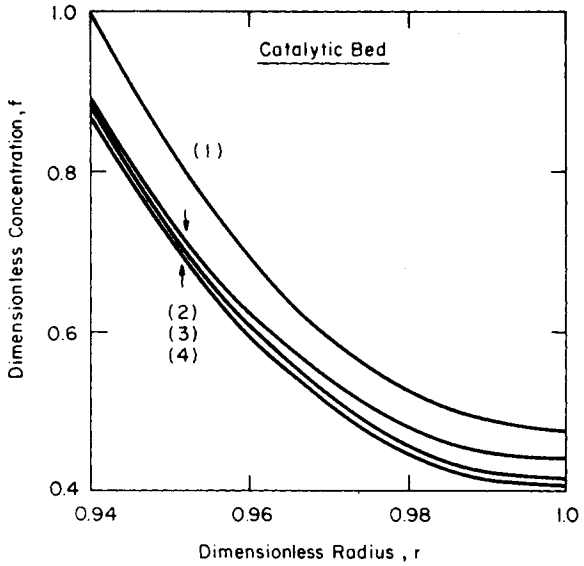

Figure 2. Effects of the initial condition on the concentration in the bed. Curve (1): initial condition; Curve (2): solution vector at $z = 0.004$ using Eq. 16 as the initial condition; Curve (3): solution vector at $z = 0.004$ using Eq. 18 as the initial condition; Curve (4): solution vector at $z = 0.01$ for both Eqs. 16 and 18 as the initial condition; Parameters are listed in Table 3.

thermal gradients never exceeded 10 K. A full discussion of the thermal gradients is given later. The thermal flux at $r = 1$ is a function of U, the overall heat transfer coefficient, which includes the shell side coefficient, which, in turn, is a function of the coolant flow rate, i.e., the coolant Reynolds number, Re_f, based on the outside diameter of the tube. The shell side heat transfer coefficient was computed from Eq. 24 (Fand, 1965),

$$Nu_f = (0.35 + 0.56\,Re_f^{0.52})Pr_f^{0.3}, \qquad (24)$$

and the thermal conductivity of the wall was taken as that for stainless steel (Eckert and Drake, 1959). For the present analysis Dowtherm A was arbitrarily chosen as the coolant.

Preliminary runs showed that the coolant Reynolds number could be varied between 50 and 200 without producing significant variations in the ABR's solution vectors using either the parabolic or the elliptic descriptions. Due to small thermal gradients and the insensitivity to the coolant Reynolds number, the shell side heat transfer coefficient was thereafter held constant at 41.84 W/m²·K, thus fixing the thermal boundary condition at $r = 1$.

Initial Condition Analysis

For the parabolic system of equations the functionality of Eq. 18 was obtained by a collocation method (Ascher et al., 1978) to solve Eqs. 19–21. The temperature was assumed constant and the dimensionless concentration in the screen was set equal to one so

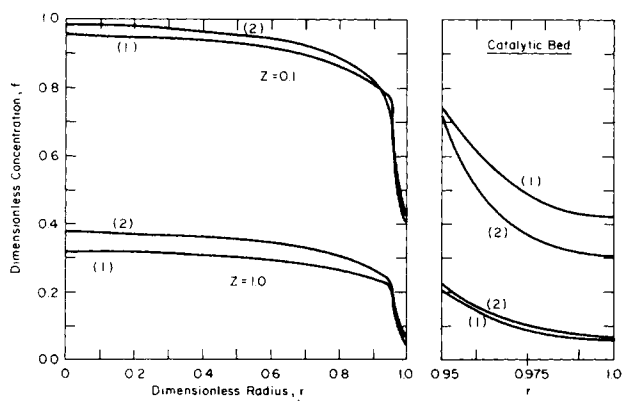

Figure 3. Effects of inert particle size in the ABR: exit radial profiles.

TABLE 3. PARAMETER DATA FOR CO METHANATION IN ABR

	Set 1	Set 2
ϵ_1	0.388	0.388
$\bar{\epsilon}$	0.426	0.398
ϵ_2	0.588	0.505
k_{mix}	0.117 W · m^{-1} · K^{-1}	0.117 W · m^{-1} · K^{-1}
d_P	1.016 cm	0.33 cm
d_P^{cat}	0.02 cm	0.02 cm
$\bar{r}_w$	2.69 cm	2.69 cm
$\bar{r}_o$	3.4 cm	3.4 cm
r_T	0.945	0.945
r_B	0.950	0.950
L/d_P	150	458
d_T/d_P	5	15
Sc	1.1	1.1
Pr	0.505	0.505
Re	143	50
T_o	573 K	573 K
t_c	1.0	1.0
H_2/CO	3	3
X_{CO}^o	0.25	0.25
P	2.17 MPa	2.17 MPa
τ_{screen}**	0.58	0.58
τ_{bed}*	0.40	0.40
ρ_B*	1.0×10^3 kg/m^3	1.0×10^3 kg/m^3

* arbitrarily set.
** from Shah and Roberts (1974).

that the two-point boundary value problem for the dimensionless concentration in the bed region was solved with the boundary conditions given by Eqs. 20 and 21.

The computed functionality of f for $r_B \le r \le 1$ at $z = 0$ can be seen in Figure 2—curve (1). The effect of the initial condition can be seen in Figure 2. At $z = 0.004$ the solution vectors for the bed are still influenced by the initial condition (curves 2 and 3) but this influence vanishes by the time $z = 0.01$ (curve 4). This "washing out" is characteristic of parabolic partial differential equations, and thus exit reactor behavior was independent of the choice of initial condition.

Effects of Inert Particle Size and Catalytic Bed Configuration Upon Reactor Performance

Figure 3 shows the exit dimensionless concentration profiles for an ABR using the parameters listed in Table 3. This figure illustrates the effect of the inert core particle size on reactor performance. The superficial velocity was held constant for this comparison. From Carberry (1976), for a radial Peclet number of 10, the number of radial mixers in a tubular packed bed is

$$\text{no. of radial mixers} = 5(d_T/d_P). \qquad (25)$$

As d_T/d_P increases so does the number of radial mixers, i.e., radial mixing decreases. To maximize radial mixing d_T/d_P should be minimized. These qualitative effects can be seen in Figure 3 for the annular bed reactor as well. At $z = 0.1$ and $z = 1.0$ the radial concentration gradient in the inner core (curve 2) for the large d_T/d_P (small particle) is greater than that for the small d_T/d_P (curve 1, large particle). At $z = 0.1$ the increased radial movement

TABLE 4. CATALYTIC BED CONFIGURATION VS. AVERAGE EXIT CONVERSION

Other Parameters As Given in Table 3, Set 1 Re = 200

r_T	r_B	L/d_P	% Conversion
0.935	0.940	150	61.7
0.945	0.950	150	57.5*
0.955	0.960	150	51.0
0.935	0.940	123	53.0*
0.955	0.960	191	61.8*

* equivalent mass of catalyst.

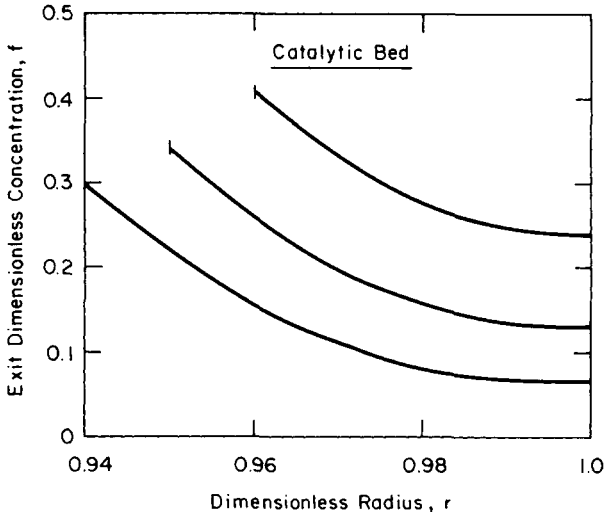

Figure 4. Influence of catalytic bed thickness on bed profiles.

brought about by the larger particles transports more material to the bed maintaining higher concentrations in this region. Since the concentration in the bed is higher, the reaction rate is faster and therefore more material can be converted. This behavior was observed through most of the reactor but as the reactants deplete the shape of the profiles varies as can be seen in Figure 3 at $z = 1.0$. Values of $d_T/d_P < 5$ were not explored, since it was anticipated that the system was no longer a continuum in this range (Carberry, 1976). From the results of Figure 3 one can see that in the ABR, larger inert particle size improved the exit conversion. Large inner core particle size was also beneficial in minimizing the pressure drop, which never exceeded 1% of the inlet pressure. The pressure drop was calculated using the Mehta and Hawley (1969) correlation.

One would expect significant variations in conversion with changing bed thickness. Table 4 shows the effects of the configuration of the catalytic bed upon the average exit conversion. Thermal gradients (axial and radial) for each case listed in Table 4 showed only 1–6 K differences. As can be seen from Table 4, minor increases in the bed thickness (at constant L/d_P) produced significant changes in the average exit conversion. The change in conversion by lowering r_B from 0.945 to 0.935 was less than that observed when r_B was decreased from 0.955 to 0.945. This behavior is better illustrated by Figure 4. As the dimensionless concentration approaches zero at the wall, increased bed thickness will have lesser effect upon the average exit conversion due to the depletion of reactant, i.e., reaction rate going to zero.

From the (*) values of Table 4, it can be seen that it was better to decrease the bed thickness and increase the reactor length, i.e., residence time. Since the radial transport to the screen is aided by

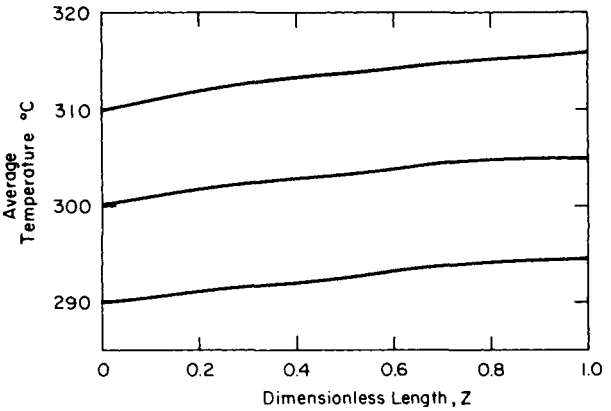

Figure 5. Axial temperature profiles: Re = 100.

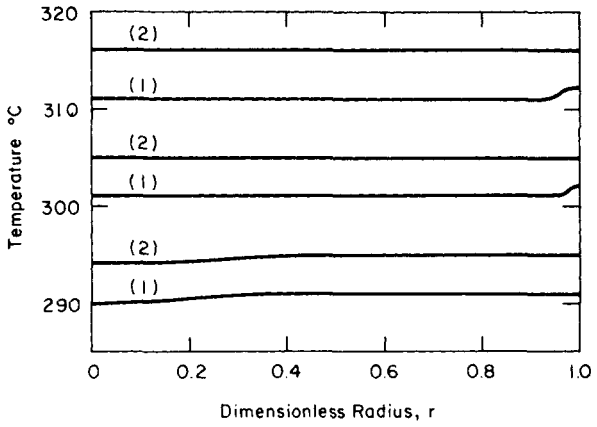

Figure 6. Radial temperature profiles: Re = 100; Curve (1): $z = 0.1$, Curve (2): $z = 1.0$.

convection and since the screen in highly porous, the transport of material to the screen-bed interface is many times faster than the radial transport in the bed. If the catalytic bed exposes more surface towards the inner core then more material can be converted per unit mass of catalyst charged into the reactor.

Effects of Inlet Temperature and Reynolds Number Upon Reactor Performance

The effects of feed temperature, T_o, and Reynolds number, Re, upon the ABR reactor performance were studied. As previously mentioned, the bulk coolant temperature was set equal to the inlet reactants temperature. The reactor performance was studied in the parameter space of $290°C \leq T_o \leq 310°C$, $75 \leq Re \leq 225$, with physical parameters from Table 3, Set 1.

Typical axial and radial temperature profiles are shown in Figures 5 and 6. From Figure 5 it can be seen that as the inlet temperature increases from 290 to 310°C the heat generation increases in the bed near the reactor inlet ($z = 0.1$) due to the higher reaction rate. Exit profiles are essentially flat for all inlet temperatures but the overall temperature increase in the axial direction of the reactor increases with increasing T_o as can be seen from Figure 6. Figure 7 is included to show that the temperature behavior of the interface of the screen and the bed parallels the av-

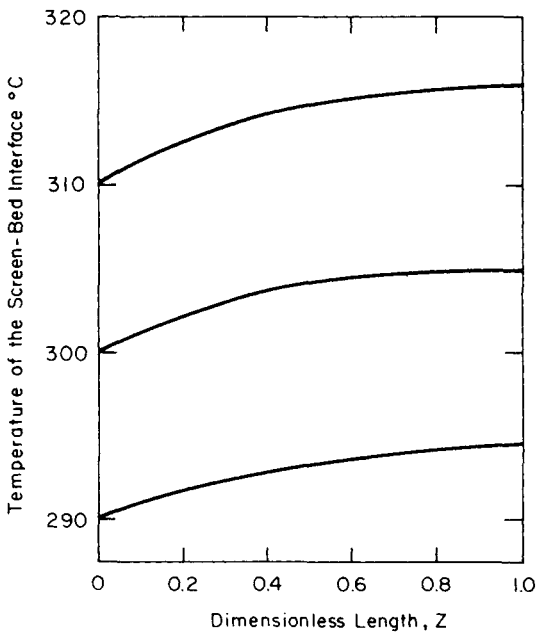

Figure 7. Axial temperature profiles of the screen-bed interface: Re = 100.

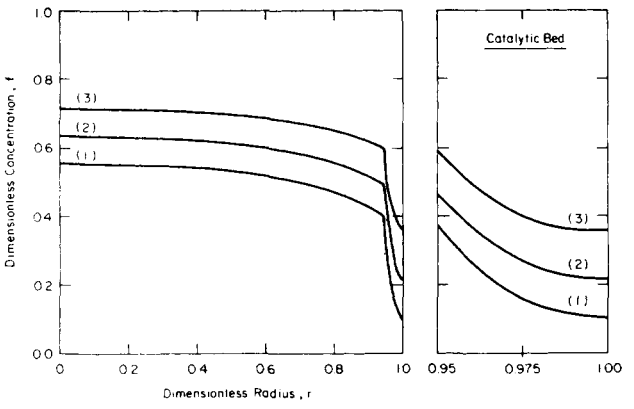

Figure 8. Radial dimensionless concentration profiles: Re = 150, z = 0.5. Feed temperature: Curve (1): 310°C, Curve (2): 300°C, Curve (3): 290°C.

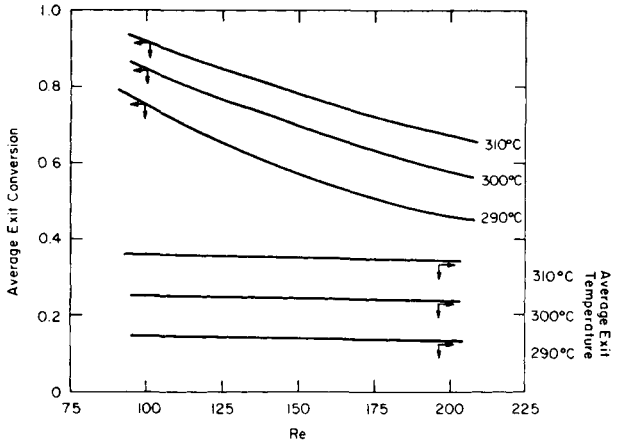

Figure 10. Average exit conversion and temperature for various Reynolds Numbers.

erage temperature behavior illustrated in Figure 6.

Typical radial and axial concentration-conversion profiles are shown in Figures 8 and 9, respectively. From Figure 8 it can be seen that an increase in feed temperature translates the radial profile downward while approximately maintaining the same shape, although slight increases in concentration drop across the bed occur with increasing temperature. Since the catalytic bed profiles were neither horizontal (reaction rate control) or equal to zero (diffusion control), the controlling mechanism in the ABR for the listed parameter space was somewhere between the limiting cases, i.e., in the coupled diffusion-reaction regime. Figure 9 shows the axial increase in conversion with feed temperature.

As previously mentioned, the ABR was essentially isothermal for the parameter space studied in that both axial and radial temperature gradients were negligible. From Figures 5, 6, and 7 it can be seen that no disadvantages in thermal behavior developed by varying feed temperature between 290°C and 310°C, but significant gains in conversion were produced by elevating this temperature. When the bed thickness was held constant, and the feed temperature was increased above 310°C, higher conversions were produced but at the expense of zero concentrations in the bed near the wall. To eliminate the zero concentrations thinner beds could be used, but since the main thrust in the development of the ABR is to provide larger amounts of catalyst than a TWR for poisoning situations, the optimal bed thickness also depends upon the poisoning rate and cannot be found from a steady-state analysis. Since only steady-state behavior was presently studied, higher temperatures where zero concentrations occur in the bed were not studied. The behavior described above holds at all Reynolds numbers between 75 and 225.

Figure 10 shows the effect of residence time, Re, on the exit temperature and conversion. As the residence time decreases, Re increasing, less time is available for reactants to diffuse into the bed and react. Therefore the conversion is lower, thus decreasing the heat generation, i.e., exit temperature of the product stream. It can also be seen from Figure 10 that increased feed temperatures do not change the behavior of the reactor, they only shift the curves upward.

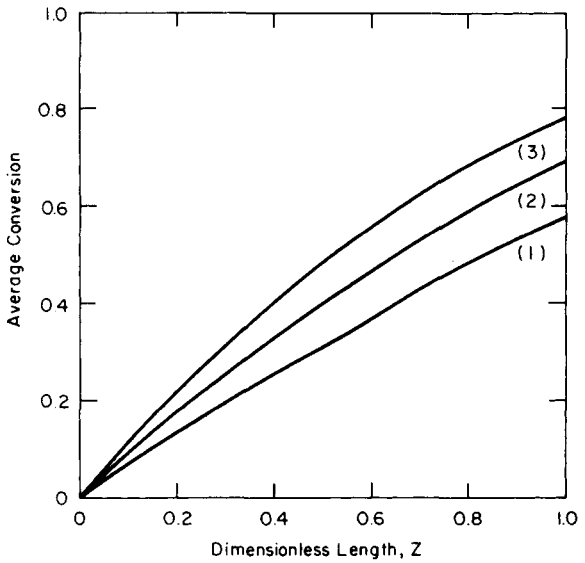

Figure 9. Axial conversion profiles: Re = 150. Feed temperature: Curve (1): 290°C, Curve (2): 300°C, Curve (3): 310°C.

CONCLUSIONS

The analysis of the annular bed reactor for the methanation of carbon monoxide using the parabolic problem has shown that:

(1) For the parameter space studied, the behavior of the reactor is near-isothermal and near-isobaric.

(2) Increasing the core inert particle size results in faster radial transport which gives rise to higher average exit conversion.

(3) The reactor behavior is very sensitive to the thickness of the catalytic bed for the same reactor length. However, a longer thin bed outperforms a shorter thick bed of the same catalyst mass in terms of the exit average conversion, and

(4) Higher Reynolds numbers, i.e., lower residence times, lower exit conversions and axial temperature gradients.

ACKNOWLEDGMENT

The authors wish to thank Dr. Graeme Fairweather of the Department of Mathematics at the University of Kentucky for his useful comments and suggestions on this work.

APPENDIX

Equation A.1 has been proposed (Fahien and Stankovic, 1979) for predicting local axial velocities in a packed bed over a wide range of tube and particle diameters as well as Reynolds numbers:

$$u/\langle u\rangle = S_r = \frac{A_1 + A_2 r_*^{(B+1)} - A_3 r_*^{(B+2)}}{A_1 + \dfrac{2A_2}{B+3} - \dfrac{2A_3}{B+4}}, \qquad \text{(A.1)}$$

$$\text{for } 0 \le r_* \le 1,$$

where

$$A_1 = \frac{1}{B+2} - \frac{\alpha - 1}{\alpha(B+1)}, \qquad \text{(A.2)}$$

$$A_2 = \alpha - 1/\alpha(B + 1), \tag{A.3}$$

$$A_3 = 1/B + 2, \tag{A.4}$$

$$B = 0.45\alpha^{1.5}, \tag{A.5}$$

$$\alpha = \bar{r}_T/d_P, \tag{A.6}$$

$$r_* = r/r_T. \tag{A.7}$$

Recently, Ahmed and Fahien (1980) proposed the following equations for predicting the local radial dispersion coefficient for mass (E):

$$E = \begin{cases} E_o + 3(E_m - E_o)\left(\dfrac{r_*}{r_{*m}}\right)^2 + 2(E_o - E_m)\left(\dfrac{r_*}{r_{*m}}\right)^3, & 0 \le r_* \le r_{*m}, \\ E_m\left(\dfrac{1 - r_*}{1 - r_{*m}}\right), & r_{*m} \le r_* \le 1, \end{cases} \tag{A.8}$$

where

$$r_{*m} = 1 - 2/\alpha, \tag{A.9}$$

$$E = \frac{6(0.5 - 0.15\,E_o {r_{*m}}^2)}{1 + r_{*m} + 0.1{r_{*m}}^2}, \tag{A.10}$$

$$E_o = (9/8)S_r(0)[1 + 4.85\alpha^{-2}], \tag{A.11}$$

and for heat (k):

$$k = \begin{cases} k_o + 3(k_m - k_o)\left(\dfrac{r_*}{r_{*m}}\right)^2 + 2(k_o - k_m)\left(\dfrac{r_*}{r_{*m}}\right)^3, & 0 \le r_* \le r_{*m}, \\ k_m - (k_m - k_w)\left(\dfrac{r_* - r_{*m}}{1 - r_{*m}}\right), & r_{*m} \le r_* \le 1, \end{cases} \tag{A.12}$$

where

$$k_m = \frac{3 - 0.9k_o r_{*m} - k_w\left(\dfrac{r_{*m}^2 - 3r_{*m} + 2}{1 - r_{*m}}\right)}{1 + r_{*m} + 0.1\,{r_{*m}}^2}, \tag{A.13}$$

and k_o, k_w, and $\langle k \rangle$ are obtained from the Argo-Smith model (1953) with the parameters evaluated at the centerline, $\frac{1}{2}\,d_P$ from the wall and the average conditions, respectively.

NOTATION

a_m = average pore radius of the catalyst pellet (m)
A_m = $L/\bar{r}_w$
A_1, A_2, A_3 = given by Eqs. A.2, A.3, and A.4
A_n = $d_P/\bar{r}_w$
B = given by Eq. A.5
C_i = concentration of species i (mol/m^3)
C_o = inlet concentration of carbon monoxide (mol/m^3)
C_{pm} = heat capacity of the reaction mixture (J/mol · K)
d_P, d_P^{cat} = diameter of the inner core packing, of the catalyst particles (m)
D_{mix} = diffusivity of the reaction mixture referred to carbon monoxide (m^2/s)
D_r, D_a = dimensionless mass dispersion coefficient for the radial and axial directions (referred to D_{mix})
E, E_o, E_m = dimensionless mass dispersion coefficient, at the center of the core, at the maximum (referred to the cross sectional average dispersion coefficient)
f = dimensionless concentration (C/C_o)
ΔH_r = heat of reaction, assumed independent of temperature (J/mol)
k_{mix} = thermal conductivity of the reaction mixture (W/m · K)
k, k_o, k_m, k_w = dimensionless radial thermal conductivity, at the center, at the maximum, at the wall, referred to $\langle k \rangle$
$\langle k \rangle$ = cross sectional average radial thermal conductivity (W/m · K)
K_o = reaction parameter given by Eq. 23
K_r, K_a = dimensionless radial and axial thermal conductivity referred to k_{mix}
L = reactor length (m)
Nu_f = Nusselt number for the coolant fluid
P = absolute pressure (kPa)
$\langle Pe \rangle$ = cross sectional average radial Peclet number for mass
Pr, Pr$_f$ = Prandtl number of the reacting fluid, of the coolant fluid
$\bar{r}$ = true radial distance (m)
$\bar{r}_w, \bar{r}_o, \bar{r}_T, \bar{r}_B$ = radius of the inside of the tube wall, of the outside of the tube wall, of the inner core-screen interface, of the screen-bed interface (m)
r = dimensionless radius, $\bar{r}/\bar{r}_w$
r_T = $\bar{r}_T/\bar{r}_w$
r_B = $\bar{r}_B/\bar{r}_w$
r_* = $\bar{r}/\bar{r}_T$ or r/r_T
r_{*m} = defined by Eq. A.9
$\mathcal{R}$ = reaction rate function (mol/m^3 · s)
R = dimensionless reaction rate, $\mathcal{R}/\mathcal{R}_o$
R_g = universal gas constant
Re = Reynolds number of the reacting fluid, $\langle u \rangle \rho_{mix} d_P/\mu_{mix}$
Re$_f$ = Reynolds number of the coolant fluid based on the outside diameter of the tube
S_r = defined by Eq. A.1
Sc = Schmidt number
T = temperature (K)
t = dimensionless temperature, T/T_o
t_c = bulk temperature of the coolant/T_o
u = point velocity (m/s)
$\langle u \rangle$ = cross sectional average velocity (m/s)
U = overall heat transfer coefficient for the tube wall and shell side convection (W/m^2 · K)
U_c = $U\bar{r}_w/k_{mix}$, dimensionless heat transfer coefficient (a Biot number)
X^o_{CO} = inlet mole fraction of carbon monoxide
$\bar{z}$ = true axial coordinate (m)
z = dimensionless axial coordinate, $\bar{z}/L$

Greek Letters

α = defined by Eq. A.6
β = Prater number, $\Delta H_r D_{mix} C_o/k_{mix} T_o$
$\epsilon_1, \bar{\epsilon}, \epsilon_2$ = void fraction, at the center of the core, the cross sectional average, at the core-screen interface
θ_{cat} = void fraction of the catalyst particles
μ_{mix} = viscosity of the reacting fluid
ρ_{mix}, ρ_B = density of the reacting fluid, the catalytic bed (kg/m^3)
τ = tortuosity factor of either the screen or bed
τ_{cat} = tortuosity factor of the catalyst pellet
ϕ = Thiele modulus, $\bar{r}_w\sqrt{\mathcal{R}_o/D_{mix}C_o}$

Superscripts

T = for the core region
sc = for the screen region
B = for the bed region

Subscripts

o = at the reactor inlet

LITERATURE CITED

Ahmed, M. and R. W. Fahien, "Tubular Reactor Design—I. Two Dimensional Model," *Chem. Eng. Sci.*, **35**, 889 (1980).

Argo, W. B. and J. M. Smith, "Heat Transfer in Packed Beds," *Chem. Eng. Prog.*, **49**, 443 (1953).

Ascher, U., J. Christiansen, and R. D. Russell, "COLSYS—A Collocation Code for Boundary Value Problems," Proceedings of Working Conference for Codes for Boundary Value Problems in ODE's, Houston, TX (May, 1978).

Carberry, J. J., *Chemical and Catalytic Reaction Engineering*, McGraw-Hill, New York (1976).

Dalla Betta, R. A., A. G. Piken, and M. J. Shelef, "Heterogeneous Methanation: Steady-State CO Hydrogenation on Supported Ruthenium, Nickel, and Rhenium," *J. of Catal.*, **40**, 173 (1975).

Davis, M. E., G. Fairweather, and J. Yamanis, "Annular Bed Reactor—Methanation of Carbon Dioxide," *Can. J. Chem. Eng.*, **59**, 497 (1981).

Davis, M. E., "Analysis of an Annular Bed Reactor for the Methanation of Carbon Oxides," Ph.D. Thesis, University of Kentucky, Lexington, Kentucky (1981).

DeBruijn, E. W., W. A. DeJong, and T. VanDerSpeigel, "Methanation in a Parallel Passage Reactor," *ACS Symp. Ser.*, No. 65, 63 (1978).

DeWasch, A. P. and G. Froment, "Heat Transfer in Packed Beds," *Chem. Eng. Sci.*, **27**, 567 (1972).

Eckert, E. R. G. and R. M. Drake, *Heat and Mass Transfer*, McGraw-Hill, New York (1959).

Fahien, R. W. and J. M. Smith, "Mass Transfer in Packed Beds," *AIChE J.*, **1**, 28 (1955).

Fahien, R. W. and I. M. Stankovic, "An Equation for the Velocity Profile in Packed Columns," *Chem. Eng. Sci.*, **34**, 1350 (1979).

Fand, R. M., "Heat Transfer by Forced Convection from a Cylinder to Water in Crossflow," *Int. J. Heat Mass Transfer*, **8**, 995 (1965).

Goodman, D. W., R. D. Kelly, T. E. Madey, and J. T. Yates, "Kinetics of the Hydrogenation of CO over a Single Crystal Nickel Catalyst," *J. of Catal.*, **44**, 226 (1980).

Haynes, W. P., R. R. Schehl, J. K. Weber, and A. J. Forney, "The Study of an Adiabatic Parallel Plate Methanation Reactor," *Ind. Eng. Chem. Proc. Des. Dev.*, **16**, 113 (1977).

Jarvi, G. A., K. B. Mayo, and C. H. Bartholomew, "Monolithic-Supported Nickel Catalysts: I. Methanation Activity Relative to Pellet Catalysts," *Chem. Eng. Commun.*, **4**, 325 (1980).

Lawson, J. D. and J. L. Morris, "The Extrapolation of First Order Methods for Parabolic Partial Differential Equations. I," *SIAM J. Numer. Anal.*, **15**, 1212 (1978).

Lindberg, B., "On Smoothing and Extrapolation for the Trapezoidal Rule," *B.I.T.*, **11**, 29 (1971).

Mehta, D. and M. C. Hawley, "Wall Effect in Packed Columns," *Ind. Eng. Chem. Proc. Des. Dev.*, **8**, 280 (1969).

Penline, H. W., R. R. Schehl, and W. P. Haynes, "Operation of a Tube Wall Methanation Reactor," *Ind. Eng. Chem. Proc. Des. Dev.*, **18**, 56 (1979).

Satterfield, C. N., *Mass Transfer in Heterogeneous Catalysis*, M.I.T. Press, Cambridge (1970).

Schuler, R. W., V. P. Stallings, and J. M. Smith, "Heat and Mass Transfer in Fixed-Bed Reactors," *CEP Symp. Ser.*, **48**(4), 28 (1952).

Schertz, W. W. and K. B. Bischoff, "Thermal and Material Transport in Nonisothermal Packed Beds," *AIChE J.*, **15**, 597 (1969).

Schwartz, C. E. and J. M. Smith, "Flow Distribution in Packed Beds," *Ind. Eng. Chem.*, **45**, 1209 (1953).

Shah, M. A. and D. Roberts, "Mass Transfer Characteristics of Stacked Metal Screens," *Adv. Chem. Ser.*, **133**, 259 (1974).

Vannice, M. A., "The Catalytic Synthesis of Hydrocarbons from H_2/CO Mixtures over the Group VIII Metals—IV. The Kinetics Behavior of CO Hydrogenation over Ni Catalysts," *J. of Catal.*, **44**, 152 (1976).

Manuscript received January 23, 1981; revision received April 30, and accepted May 15, 1981

Diffusional Influences on Deactivation Rates: Experimental Verification

The internal diffusion-deactivation model of Krishnaswamy and Kittrell (1981a) is tested and verified by using laboratory deactivation data on the decomposition of hydrogen peroxide by immobilized catalase. Through an analysis of the influence of diffusional phenomena on the deactivation kinetics, estimates of the intrinsic deactivation rate constant have also been provided.

S. KRISHNASWAMY

and

J. R. KITTRELL

Department of Chemical Engineering
University of Massachusetts
Amherst, MA 01003

SCOPE

Deactivation effects can be masked by diffusion in catalyst particles leading to erroneous measurements of deactivation rate constants from laboratory data. Effective measurements of intrinsic deactivation rate constants are, however, required for development of generalized theories of deactivation and reactor design. Computer solutions have been developed for a few problems in this category, but the solutions are so complex that they have not been generally applied to experimental deactivation data.

In a recent theoretical study, Krishnaswamy and Kittrell (1981) developed a model descriptive of deactivation data exhibiting the masking effects of internal diffusion, for the case of first order reaction with first order concentration-independent deactivation. The present experimental study was undertaken to examine the applicability of the model to deactivation data. For this purpose, data taken on the decomposition of hydrogen peroxide by immobilized catalase were used to test the theoretical developments.

S. Krishnaswamy is with Gulf Research & Development Co.; Harmarville, PA.